Inorganic Chemistry

Communication

pubs.acs.org/IC

Substituent-Modulated Assembly Formation: An Approach to Enhancing the Photostability of Photoelectric-Sensitive Chalcogenide-Based Ion-Pair Hybrids

Jian Lin,[†] Zhixing Fu,[†] Jiaxu Zhang,[†] Yujia Zhu,[†] Dandan Hu,[†] Dongsheng Li,[‡] and Tao Wu*[,†]

[†]College of Chemistry, Chemical Engineering and Materials Science, Soochow University, Suzhou, Jiangsu 215123, China

[‡]College of Materials and Chemical Engineering, Hubei Provincial Collaborative Innovation Center for New Energy Microgrid, Key Laboratory of Inorganic Nonmetallic Crystalline and Energy Conversion Materials, China Three Gorges University, Yichang, Hubei 443002, China

Supporting Information

ABSTRACT: A series of electronically active viologen dications (RV) with tunable substituent groups were utilized to hybridize with $[Ge_4S_{10}]^{4-}$ (T2 cluster) to form the hybrids of **T2@RV**. These hybrids exhibited variable supermolecular assembly formation, tunable optical absorption properties, and different photoelectric response under the influence of different RV dications. Raman testing and time-dependent photocurrent response indicated that the photosensitivity and photostability of **T2@RV** could be integrated while choosing suitable RV dications. Current research provides a general method to build a tunable hybrid system based on crystalline metal chalcogenide compounds through the replacement of photoinactive cationic organic templates with photoactive ones with different substituent groups.

Inorganic−organic hybridization is one of the most effective methods to functionalize inorganic and/or organic units through synergistic interactions. During the past decades, a large number of hybrid crystalline metal chalcogenides (CMCs) have been synthesized through a hybridization strategy. Such hybrid CMCs with structural diversity and tunability of the composition and electronic structure exhibit potential and practical applications in photoluminescence, as catalysts, as sensors, in ion conducting, and so on.[1−8] It should be noted that most of the CMCs with variable geometry structures as well as tunable electronic structures contain organic templates and/or structure-directing agents (SDAs). These templates in the CMCs only functioned as either charge-balancing or space-filling agents. Poor electric activities of SDAs to some extent deteriorate the photoelectric properties of these solid-state CMCs. Intentionally integrating electronically active organic components into CMCs is an alternative method to further ameliorate their electric properties. In order to stabilize the negatively charged inorganic components and integrate the organic functional unit, positively charged electronically active organic molecules are welcomed in most of the electron-rich CMCs. Viologens are well-known electronically active organic molecules that are frequently used as a cation electron acceptor to prepare inorganic−organic hybrids. These hybrids generally exhibit some novel properties, such as electro/photochromism, ferroelectricity, and electron-transfer indicator or stabilizer.[9−15] Moreover, it is very easy to systematically construct inorganic−organic hybrids through alteration of the substituted group of viologen.[16−18] Actually, viologens are likely to hybridize with metal chalcogenides because of their strong ion-pair interactions.[19,20] For example, influenced by electronically active viologen, hybrid chalcogenidometalates show dramatic red shifts in their absorption spectra as well as improved stability compared with traditional-metal chalcogenides.[19,21]

Generally, the inorganic parts in the reported hybrid CMCs are either electrically neutral or negatively charged. They are usually protected by covalently bonded organic ligands, which are detrimental to the electron-related process. However, for the negatively charged metal chalcongenide nanocluster without a covalent organic ligand, they are vulnerable to external attacks, such as light illumination and/or oxidation.[22,23] In order to simultaneously reserve the electric sensitivity and stability of electronegatively charged metal chalcogenide clusters, well-designed photoactive countercations are necessary. As one of the well-known negatively charged semiconductor clusters with high stability and solubility in water, $[Ge_4S_{10}]^{4-}$ was ever selected as a secondary building unit for the construction of many hybrids.[24−28] Recently, Dai's group reported three hybrid thiogermanates based on methylviologen cations ($[MV]_2(Ge_4S_{10})\cdot Sol$ (denoted as **T2@MV**), which show solvent-induced color changes and switchable fluorescent emission as well as photoelectric responsive properties.[29] However, the photoelectric response of **T2@MV** exhibits a clear decay even in the 400 s interval irradiation. The combination of the photoelectric sensitivity of hybrids and photostability is of fundamental importance to endow them with potential applications in optoelectronic devices.

In this manuscript, we applied electron-poor viologen dications with different substituent groups (denoted as RV; the synthetic method is shown in Scheme S1 and the Supporting Information, SI) to construct a series of $[Ge_4S_{10}]^{4-}$ cluster (T2)-based hybrid compounds (denoted as **T2@RV**). Under the influence of steric hindrance from RV with different substituent groups (MV = methyl viologen, EV = ethyl viologen, n-BV = butyl viologen, AV = amyl viologen, and BV = benzyl viologen),

Received: December 18, 2016
Published: February 28, 2017

DOI: 10.1021/acs.inorgchem.6b03061
Inorg. Chem. 2017, 56, 3119−3122

T2@RV compounds exhibit different assembly formation and diverse photoelectric sensitivity and photostability. Suitable substituent groups in **T2@RV** finally give rise to combined photoelectric sensitivity and photostability in hybrid chalcogenidometalates.

Crystalline ion-pair hybrids of **T2@RV** were prepared at room temperature (see the SI). The structure refinement results are summarized in Table S3. Single-crystal X-ray diffraction (XRD) analyses show that **T2@RV** consists of a discrete $[Ge_4S_{10}]^{4-}$ cluster and two RV dications. Because of different substituent groups on the RV, **T2@RV** exhibits variable assembly formation. For hybrids of $(MV)_2{\cdot}[Ge_4S_{10}]$ (now denoted as **T2@MV-1** and **T2@MV-2**), they have structure packing patterns similar to that reported in the literature.[29] As shown in Figure S1, two MV^{2+} cations look like "electron locks" around the corner of the T2 nanocluster in **T2@MV-1**, and strong ion-pair interactions exist between the $[Ge_4S_{10}]^{4-}$ cluster and MV^{2+} because the S···N distance (3.479 Å) is short. However, such MV^{2+} cations show weak interaction (the S···N distance is 4.001 Å) with neighboring T2 clusters in the crystal lattice. Compared with **T2@MV-1**, **T2@MV-2** exhibits lower structure symmetry and weaker ion-pair interactions (Figure S2). With an increase of the alkyl chain length in RV, **T2@EV** and **T2@n-BV** exhibit poor crystallinity during the supermolecular self-assembly process. Single-crystal structure analysis indicates that **T2@EV** shows low symmetry and weak ion-pair interaction as well (Figure S3). As shown in Figure 1, a negatively charged T2 cluster is surrounded by four n-BV dications. The S···N distance between each terminal sulfur atom in the T2 cluster and the positively charged nitrogen center in n-BV is 3.454 Å (Figure 1a). Four such n-BV dications further interact with four other T2 clusters to pack into a 3D supermolecular framework through ion-pair interactions (Figure 1b,c). Abundant free space in the sublattice framework is filled with five other types of sublattice frameworks (Figure 1d). The S···N distance in the two closest sublattices is 4.327 Å (Figure S4).

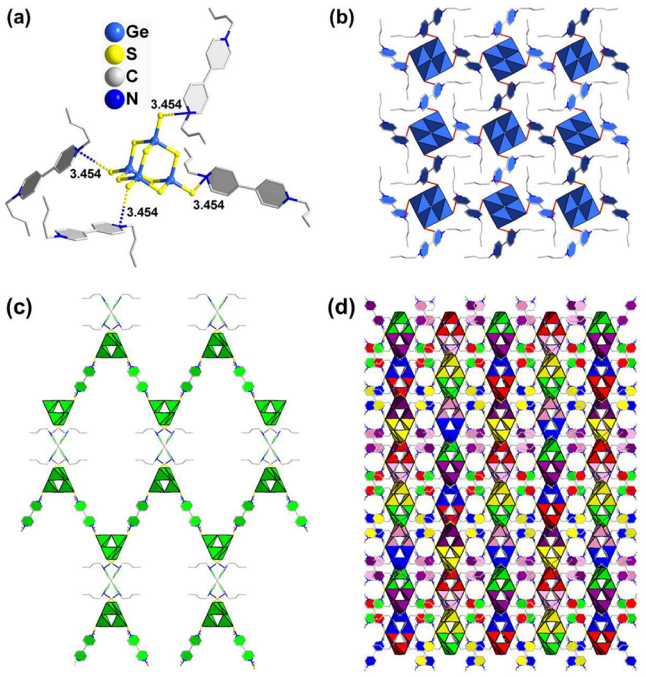

Figure 1. (a) Interaction between the T2 cluster and four n-BV dications. (b) Packing structure of an ion-pair hybrid of **T2@n-BV** viewed from the *b* axis. (c) One type of supermolecular sublattice framework of **T2@n-BV** viewed from the [110] direction. (d) 6-fold crossed supermolecular framework of **T2@n-BV** viewed from the [110] direction.

When the alkyl chain length of RV increases or a more rigid benzene ring is added on the RV, the hybrids of **T2@AV** and **T2@BV** are obtained, respectively. Direct mixing of an aqueous solution of the T2 cluster and an AV dication salt can lead to the formation of crystals of **T2@AV** in a few seconds. By contrast, the reaction of T2 and BV ions in the aqueous solution is much faster, which only produces crystalline powders. Crystals of **T2@BV** are obtained by a diffusion method (see the SI). Hybrids of **T2@AV** and **T2@BV** crystallize in the same tetragonal space group ($P42/n$) with **T2@n-BV**. They also exhibit an assembly formation similar to that of **T2@n-BV**. The anionic T2 nanocluster is surrounded by four AV and BV molecular dications in **T2@AV** and **T2@BV**, respectively. Also, the S···N distances between the T2 cluster and AV and BV dications are 3.493 and 3.773 Å, respectively (Figures S5a and S6a). The T2 clusters could also interact with AV and BV molecular cations to form a 3D supermolecular framework (Figures S5 and S6). Densely packed ion-pair hybrids of **T2@AV** and **T2@BV** could be realized by interpenetrating six sublattices of the 3D supermolecular framework. In contrast to **T2@n-BV**, the S···N distance between the two closest sublattices in **T2@AV** and **T2@BV** is further increased (Figures S5e and S6e). Although the ion-pair interactions between neighboring sublattice frameworks in **T2@AV** and **T2@BV** are much weaker than those in **T2@n-BV**, the long-alkyl-chain and rigid substituent in AV and BV could provide more steric hindrance to anchor the flexible sublattice framework, which may be responsible for the good quality of the crystallinity.

The phase purity of **T2@RV** was examined by powder XRD measurements by comparing the XRD patterns of as-synthesized samples with the simulated ones from single-crystal data (Figure S7). UV−vis diffuse-reflectance spectroscopy (DRS) measurements were also performed to determine the optical band gap. Owing to the influence by different substituents, the optical absorption edge of RV varied from 2.75 to 3.35 eV (Figure S8). The optical absorption edge of **T2@RV** exhibits a large red shift compared with the pristine **T2@PR** (PR is the abbreviation of piperidine), which may be explained by the introduction of electronically active viologen and charge-transfer-related absorption (Figure 2). The charge-transfer band gap of **T2@RV** decreased from 2.50 to 1.75 eV with an increase of the alky chain length of RV. For **T2@BV**, the band gap is 2.25 eV.

Besides the optical absorption properties, the photoelectric conversion properties as well as the photostability of **T2@RV** were also investigated in a photoelctrochemical cell with a three-electrode setup (a more detailed description is given in the SI). As presented in Figure S9, the background photocurrent of indium−tin oxide (ITO) is 0.04 $\mu A/cm^3$, which is far below the value of a **T2@RV**-modified ITO working electrode. While the biased potential is set at 0.5 V, the **T2@MV-1**-decorated photoelectrode generates a good photocurrent, comparable with the results reported in the literature (Figure 3).[29] However, the photocurrent density of **T2@MV-1** exhibits an observable decrease after 30 cycles in 600 s. After long-time irradiation, the photocurrent density of **T2@MV-1** was reduced to one-third of its original value (inset in Figure 3). As for the **T2@AV**-modified photoelectrode, it exhibits photostability similar to that of **T2@MV-1** (Figure S10). When the alkyl group was replaced by the benzyl group, the photostability of **T2@BV** was

DOI: 10.1021/acs.inorgchem.6b03061
Inorg. Chem. 2017, 56, 3119−3122

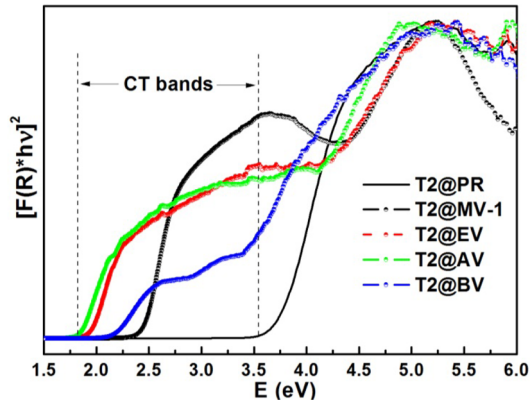

Figure 2. Tauc plots of ion-pair hybrids **T2@PR** and **T2@RV** derived from UV−vis DRS.

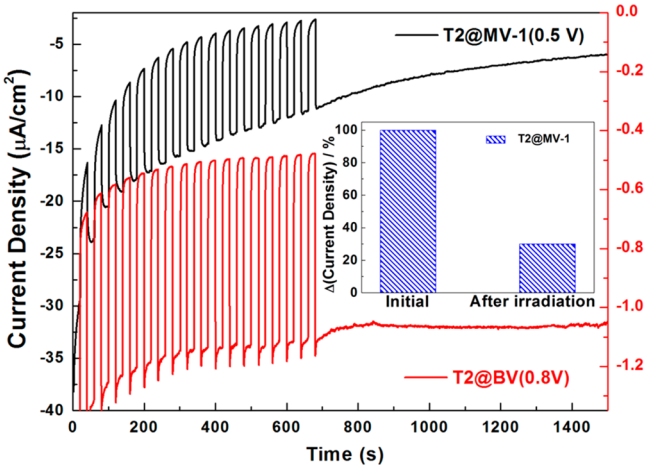

Figure 3. Photocurrent responses of **T2@MV-1** (black line) and **T2@BV** (red line) in light on-off irradiation with applied potentials at 0.5 and 0.8 V, respectively. Inset: Photoelectric response of **T2@MV-1** after long-time irradiation.

significantly improved. As shown in Figure 3, the photocurrent repeatability of **T2@BV** was proven by not only the 30 cycles of light on−off processes but also the continuous long-time irradiation. By increasing the applied potential on the **T2@BV**-modified photoelectrode from 0.5 to 0.8 V, the photocurrent density of **T2@BV** increased as well (Figure S10b). Moreover, the photostability of the **T2@RV** samples were also verified by Raman testing. As shown in Figure S11a, the Raman signals of **T2@PR**, **T2@AV**, and **T2@BV** are clearly detectable under the 785 nm laser irradiation (class IIIB laser, 5−500 mW). The signals from an optically active inorganic T2 cluster in the short-wavelength region are distinguished from the ones from the AV and BV organic dications in the high-energy region.[24] However, the Raman signal of **T2@MV-1** totally disappeared under excitation of the 785 nm laser (Figure S11b). An obvious color change is also observed, indicating that it decomposed instantly upon exposure to laser irradiation (inset in Figure S11b).

On the basis of the above results, it is obviously observed that the photosensitivity and photostability of hybrids of **T2@RV** are greatly influenced by the structure diversity. The potential charge-transfer efficiency can be regulated by the potential charge-transfer pathway, i.e., the nearest S···N distance in the **T2@RV**, which is influenced by the length of the substituent groups. For a longer S···N distance between the RV and T2 clusters, higher voltage needs to be applied on the **T2@RV**-decorated photoelectrode in order to produce the appropriate photocurrent. Nevertheless, the relatively short alkyl group, such as the ones appearing in **T2@MV-1**, **T2@EV**, and **T2@n-BV**, cannot provide enough steric hindrance to resist photodegradation. A moderate charge-transfer pathway as well as the effective protection on the optically active units throughout the whole crystal lattice is very helpful for the real application of light-stimuli-responsive materials. In our case, a hybrid ion-pair compound of **T2@BV** is a potential candidate as a light-sensitive material because it can not only provide a moderate photocurrent but also offer well protection on the optically active unit $[Ge_4S_{10}]^{4-}$ clusters.

In summary, a series of ion-pair hybrids of **T2@RV** have been synthesized by integrating electronically active organic viologen dications with $[Ge_4S_{10}]^{4-}$ cluster-based chalcogenidometalates. Under the influence of RV dications with varied substituent groups, **T2@RV** compounds exhibit different supermolecular assembly formation and tunable optical absorption properties and different photosensitivity and photostability. This work provides a general method to stabilize and explore optically active units in a variety of chalcogenide cluster-based anionic structures through the replacement of electronically inactive organic templates by active viologen dications derivatives.

■ ASSOCIATED CONTENT

Supporting Information

The Supporting Information is available free of charge on the ACS Publications website at DOI: 10.1021/acs.inorgchem.6b03061.

X-ray crystallographic data in CIF format (CIF)

General methods, tables for the results of single-crystal data and elemental analysis, extra figures, powder XRD, absorption as well as photocurrent response, and Raman spectra (PDF)

■ AUTHOR INFORMATION

Corresponding Author

*E-mail: wutao@suda.edu.cn.

ORCID

Dongsheng Li: 0000-0003-1283-6334

Tao Wu: 0000-0003-4443-1227

Notes

The authors declare no competing financial interest.

■ ACKNOWLEDGMENTS

We acknowledge financial support from the National Natural Science Foundation of China (Grants 21271135 and 21671142), Jiangsu Province Natural Science Fund for Distinguished Young Scholars (BK20160006), a start-up fund (Q410900712) from Soochow University, the Priority Academic Program Development of Jiangsu Higher Education Institutions, Young Thousand Talented Program, and a graduate student fund (KYZZ15_0323) from Scientific Research Innovation Projects of Jiangsu Province.

■ REFERENCES

(1) Zheng, N.; Bu, X.; Wang, B.; Feng, P. Microporous and photoluminescent chalcogenide zeolite analogs. *Science* **2002**, *298*, 2366−2369.

(2) Manos, M. J.; Iyer, R. G.; Quarez, E.; Liao, J. H.; Kanatzidis, M. G. $\{Sn[Zn_4Sn_4S_{17}]\}^{6-}$: a robust open framework based on metal-linked

DOI: 10.1021/acs.inorgchem.6b03061
Inorg. Chem. 2017, 56, 3119−3122

penta-supertetrahedral $[Zn_4Sn_4S_{17}]^{10-}$ clusters with ion-exchange properties. *Angew. Chem., Int. Ed.* **2005**, *44*, 3552−3555.
(3) Zheng, N.; Bu, X. H.; Vu, H.; Feng, P. Y. Open-framework chalcogenides as visible-light photocatalysts for hydrogen generation from water. *Angew. Chem., Int. Ed.* **2005**, *44*, 5299−5303.
(4) Zheng, N. F.; Bu, X. H.; Feng, P. Y. Synthetic design of crystalline inorganic chalcogenides exhibiting fast-ion conductivity. *Nature* **2003**, *426*, 428−432.
(5) Feng, P. Y.; Bu, X. H.; Zheng, N. F. The interface chemistry between chalcogenide clusters and open framework chalcogenides. *Acc. Chem. Res.* **2005**, *38*, 293−303.
(6) Xiong, W. W.; Miao, J. W.; Ye, K. Q.; Wang, Y.; Liu, B.; Zhang, Q. C. Threading chalcogenide layers with polymer chains. *Angew. Chem., Int. Ed.* **2014**, *54*, 546−550.
(7) Xiong, W. W.; Zhang, Q. C. Surfactants as promising media for the preparation of crystalline inorganic materials. *Angew. Chem., Int. Ed.* **2015**, *54*, 11616−11623.
(8) Xiong, W. W.; Zhang, G. D.; Zhang, Q. C. New strategies to prepare crystalline chalcogenides. *Inorg. Chem. Front.* **2014**, *1*, 292−301.
(9) Huang, Y. D.; Huo, P.; Shao, M. Y.; Yin, J. X.; Shen, W. C.; Zhu, Q. Y.; Dai, J. A new type of charge-transfer salts based on tetrathiafulvalene-tetracarboxylate coordination polymers and methyl viologen. *Inorg. Chem.* **2014**, *53*, 3480−2487.
(10) Kanazawa, K.; Nakamura, K.; Kobayashi, N. Electroswitching of emission and coloration with quick response and high reversibility in an electrochemical cell. *Chem. - Asian J.* **2012**, *7*, 2551−2554.
(11) Kim, C. S.; Lee, S.; Tinker, L. L.; Bernhard, S.; Loo, Y. L. Cobaltocene-doped viologen as functional components in organic electronics. *Chem. Mater.* **2009**, *21*, 4583−4588.
(12) Leblanc, N.; Mercier, N.; Zorina, L.; Simonov, S.; Auban-Senzier, P.; Pasquier, C. Large spontaneous polarization and clear hysteresis loop of a room-temperature hybrid ferroelectric based on mixed-halide $[BiI_3Cl_2]$ polar chains and methylviologen dication. *J. Am. Chem. Soc.* **2011**, *133*, 14924−14927.
(13) Lin, R. G.; Xu, G.; Lu, G.; Wang, M. S.; Li, P. X.; Guo, G. C. Photochromic hybrid containing in situ-generated benzyl viologen and novel trinuclear $[Bi_3Cl_{14}]^{5-}$: improved photoresponsive behavior by the $\pi\cdots\pi$ interactions and size effect of inorganic oligomer. *Inorg. Chem.* **2014**, *53*, 5538−5545.
(14) Lin, R. G.; Xu, G.; Wang, M. S.; Lu, G.; Li, P. X.; Guo, G. C. Improved photochromic properties on viologen-based inorganic-organic hybrids by using π-conjugated substituents as electron donors and stabilizers. *Inorg. Chem.* **2013**, *52*, 1199−2005.
(15) Bose, A.; He, P. G.; Liu, C.; Ellman, B. D.; Twieg, R. J.; Huang, S. P. D. Strong electron-acceptor methylviologen dications confined in a 2D inorganic host: Synthesis, structural characterization, charge transport and electrochemical properties of $(MV)_{0.25}V_2O_5$. *J. Am. Chem. Soc.* **2002**, *124*, 4−5.
(16) Qiao, Y. Z.; Fu, W. Z.; Yue, J. M.; Liu, X. C.; Niu, Y. Y.; Hou, H. W. Role of cooperative templates in the self-assembly process of microporous structures: syntheses and characterization of 12 new silver halide/thiocyanate supramolecular polymers. *CrystEngComm* **2012**, *14*, 3241−3249.
(17) Ross, J. H.; Krieger, R. I. Synthesis and properties of paraquat (methyl viologen) and other herbicidal alkyl homologs. *J. Agric. Food Chem.* **1980**, *28*, 1026−1031.
(18) Huo, P.; Xue, L. J.; Li, Y. H.; Chen, T.; Yu, L.; Zhu, Q. Y.; Dai, J. Effects of alkyl chain length on film morphologies and photocurrent responses of tetrathiafulvalene-bipyridinium charge-transfer salts: a study in terms of structures. *CrystEngComm* **2016**, *18*, 2894−2900.
(19) Zhang, Q. C.; Wu, T.; Bu, X. H.; Tran, T.; Feng, P. Y. Ion pair charge-transfer salts based on metal chalcogenide clusters and methyl viologen cations. *Chem. Mater.* **2008**, *20*, 4170−4172.
(20) Jiang, J. B.; Huo, P.; Wang, P.; Wu, Y. Y.; Bian, G. Q.; Zhu, Q. Y.; Dai, J. Synthesis and photocurrent responsive properties of CdS/Se clusters integrated with methylviologen. *J. Mater. Chem. C* **2014**, *2*, 2528−2533.
(21) Kiriya, D.; Tosun, M.; Zhao, P.; Kang, J. S.; Javey, A. Air-stable surface charge transfer doping of MoS_2 by benzyl viologen. *J. Am. Chem. Soc.* **2014**, *136*, 7853−7856.
(22) Zimmermann, C.; Melullis, M.; Dehnen, S. Reactivity of chalcogenostannate salts: unusual synthesis and structure of a compound containing ternary cluster anions $[Co_4(\mu_4\text{-Se})(SnSe_4)_4]^{10-}$. *Angew. Chem., Int. Ed.* **2002**, *41* (22), 4269−4272.
(23) Palchik, O.; Iyer, R. G.; Canlas, C. G.; Weliky, D. P.; Kanatzidis, M. G. $K_{10}M_4M'_4S_{17}$ (M = Mn, Fe, Co, Zn; M′ = Sn, Ge) and $Cs_{10}Cd_4Sn_4S_{17}$: compounds with a discrete supertetrahedral cluster. *Z. Anorg. Allg. Chem.* **2004**, *630*, 2237−2247.
(24) Bonhomme, F.; Kanatzidis, M. G. Structurally characterized mesostructured hybrid surfactant-inorganic lamellar phases containing the adamantane $[Ge_4S_{10}]^{4+}$ anion: synthesis and properties. *Chem. Mater.* **1998**, *10*, 1153−1159.
(25) Liang, J. J.; Zhao, J.; Tang, W. W.; Zhang, Y.; Jia, D. X. Ethylene polyamine influence on the transition metal thiogermanates: solvothermal syntheses and characterizations of $[Ni(trien)_2]_2Ge_4S_{10}$ and $[\{Ni(tepa)\}_2(\mu\text{-}Ge_2S_6)]$. *Inorg. Chem. Commun.* **2011**, *14* (6), 1023−1026.
(26) Liu, G. N.; Lin, J. D.; Xu, Z. N.; Liu, Z. F.; Guo, G. C.; Huang, J. S. Spontaneous resolution of a new thiogermanate containing chiral binuclear nickel(II) complexes with achiral triethylenetetramine ligands: a unique water-mediated supramolecular hybrid helix. *Cryst. Growth Des.* **2011**, *11* (8), 3318−3322.
(27) Wang, M. S.; Chen, W. T.; Cai, L. Z.; Zhou, G. W.; Guo, G. C.; Huang, J. S. An inorganic-organic hybrid supramolecular hydrogen-bonding and π-π stacking network containing $Ge_4S_{10}^{4-}$ cluster: synthesis and characterization of $(H_2bipy)_2Ge_4S_{10}\cdot(bipy)\cdot 7H_2O$ (bipy = 4,4′-bipy). *J. Cluster Sci.* **2003**, *14* (4), 495−504.
(28) Rangan, K. K.; Kanatzidis, M. G. Mesolamellar thiogermanates $[C_nH_{2n+1}NH_3]_4Ge_4S_{10}$. *Inorg. Chim. Acta* **2004**, *357* (13), 4036−4044.
(29) Sun, X. L.; Zhu, Q. Y.; Mu, W. Q.; Qian, L. W.; Yu, L.; Wu, J.; Bian, G. Q.; Dai, J. Ion pair charge-transfer thiogermanate salts $[MV]_2Ge_4S_{10}\cdot$ xSol: solvent induced crystal transformation and photocurrent responsive properties. *Dalton Trans.* **2014**, *43*, 12582−12589.

DOI: 10.1021/acs.inorgchem.6b03061
Inorg. Chem. 2017, 56, 3119−3122